Environmental Science: Atmospheres

ROYAL SOCIETY OF CHEMISTRY

PAPER

View Article Online
View Journal | View Issue

Cite this: *Environ. Sci.: Atmos.*, 2022, **2**, 202

Hygroscopicity of internally mixed ammonium sulfate and secondary organic aerosol particles formed at low and high relative humidity†

Patricia N. Razafindrambinina, [a] Kotiba A. Malek, [b] Joseph Nelson Dawson,[c] Kristin DiMonte,[c] Timothy M. Raymond,[e] Dabrina D. Dutcher, [ef] Miriam Arak Freedman [cd] and Akua Asa-Awuku *[ab]

Volatile organic matter suspended in the atmosphere such as α-pinene and β-caryophyllene undergoes aging processes and chemical, and photo-oxidation reactions to create secondary organic aerosols (SOAs), which can influence the indirect effect of aerosol particles and the radiative budget. The presence and impact of water vapor and ammonium sulfate (ubiquitous species in the atmosphere) on the hygroscopicity and CCN activity of SOA have not been well characterized. In this research, three water-uptake measurement methods, cavity ring-down spectroscopy (CRD), humidified tandem differential mobility analysis (HTDMA), and cloud condensation nuclei counting (CCNC), were employed to study the hygroscopicity of α-pinene and β-caryophyllene SOAs formed by dark ozonolysis. We observed the changes in water uptake of SOAs in the absence and presence of water vapor at ~70% RH and ammonium sulfate seeds. Measured hygroscopicity was represented by a single hygroscopicity parameter (κ). Sesquiterpene SOA was observed to be insoluble, hydrophobic, and non-hygroscopic under all experimental conditions and at all initial concentrations, as β-caryophyllene SOA exhibited non-hygroscopic properties with values that were effectively 0. Conversely, monoterpene SOA water uptake is sensitive to increasing RH in the chamber during secondary aerosol formation. Dry and wet seeded monoterpene SOA showed a similar trend of increase despite variability in initial precursor concentrations. We conclude that differences in the viscosity, solubility and hydrophobicity of SOAs may be the primary factor that leads to changes in SOA hygroscopicity formed under low and high relative humidity conditions.

Received 25th August 2021
Accepted 4th January 2022

DOI: 10.1039/d1ea00069a

rsc.li/esatmospheres

Environmental significance

Hygroscopicity of atmospheric aerosol particles governs the formation of droplets, clouds, and haze that can absorb, refract, or reflect radiation, indirectly influencing the Earth's net radiative budget. Hygroscopicity, and therefore the optical properties of atmospheric droplets are dependent on particle composition and relative humidity. In this research, we probed the effects of humidity and presence of ammonium sulfate seeds on the secondary organic aerosol (SOA) hygroscopicity from α-pinene and β-caryophyllene ozonolysis, two prevalent atmospheric terpenes. The results indicate that mixed organic–inorganic aerosols formed in high humidity regions may have different water-uptake properties than those in arid regions; and the hygroscopicity differences are more pronounced for monoterpene SOA mixtures compared to sesquiterpene SOA mixtures. The reported results contribute to the body of scientific knowledge on aerosol water-uptake that reduces uncertainty in climate models.

[a]*Department of Chemistry and Biochemistry, University of Maryland, College Park, MD 20742, USA. E-mail: asaawuku@umd.edu*

[b]*Department of Chemical and Biomolecular Engineering, University of Maryland, College Park, MD 20742, USA*

[c]*Department of Chemistry, The Pennsylvania State University, University Park, PA 16802, USA. E-mail: maf43@psu.edu*

[d]*Department of Meteorology and Atmospheric Science, The Pennsylvania State University, University Park, PA 16802, USA*

[e]*Department of Chemical Engineering, Bucknell University, Lewisburg, PA 17837, USA. E-mail: ddd014@bucknell.edu; traymond@bucknell.edu*

[f]*Department of Chemistry, Bucknell University, Lewisburg, PA 17837, USA*

† Electronic supplementary information (ESI) available: Detailed experimental procedures, and figures and tables showing data analysis. See DOI: 10.1039/d1ea00069a

1 Introduction

Aerosol particles are liquid or solid particles suspended in air and are known to take up water from the atmosphere. Water uptake properties of aerosol particles can influence the aerosol particle's atmospheric lifetime, reactivity, and chemistry.[1] In addition, water uptake by aerosol particles under subsaturated conditions can affect visibility, whereas, particles can serve as cloud condensation nuclei (CCN) under supersaturated conditions. As such, the hygroscopicity of aerosol particles can contribute to the indirect radiative forcing of the Earth's climate.[2] However, the magnitude of the indirect effect of

aerosols on the total radiative budget remains uncertain, partly due to the composition, temporal, and spatial variance of atmospheric aerosol particles.[3]

Atmospheric aerosol particles can be organic or inorganic, but usually exist as a mixture of both.[4] The hygroscopicity of inorganic aerosol particles such as ammonium sulfate under sub- and supersaturated conditions has been well characterized and has been used as a calibration standard for various water uptake measurement methods.[5,6]

Organic aerosol particles can represent up to 50% of the aerosol mass.[7] Volatile organic compounds (VOCs) in the atmosphere typically exist in the gas phase and can undergo various reactions in the atmosphere (*i.e.*, photooxidation, ozonolysis, and aging) to form aerosol-phase secondary organic aerosol particles (SOAs).[8–12] VOCs include monoterpenes such as α-pinene and sesquiterpenes such as β-caryophyllene. α-Pinene is the most prevalent monoterpene (up to 35%), and arguably one of the most important biogenic SOA precursors.[13] In contrast, β-caryophyllene is less abundant but produces higher SOA yields, and thus the contribution of β-caryophyllene SOA can be significant.[14,15] SOAs from various precursors such as α-pinene and β-caryophyllene can have a range of physical and chemical properties such as O : C ratios, molecular weight, and hygroscopicity, which can affect their contributions to the net radiative forcing.

The ability of biogenic SOA to take up water and form droplets has been of interest for some time. Researchers have explored the water uptake of SOAs from various precursors and probed the effects off sub- and supersaturated conditions, mixing states, and the presence of an inorganic seed. The list of relevant references for water uptake of SOA studies similar to the systems presented here include (but are not limited to) those presented in Table 1.

Particle hygroscopicity can be represented by the parameter κ, which can be compared over saturation conditions and measurement methods.[6,25,26] It has been reported that κ-values of monoterpene and sesquiterpene may vary between supersaturated and subsaturated measurements due to partial dissolution and surface tension.[25,27] However, others have also reported that α-pinene and β-caryophyllene SOAs are dissolved during droplet activation. Therefore hygroscopicity at supersaturation was not limited by solubility but was instead driven by molecular weight: α-pinene, the precursor with a lower molecular weight, was observed to be more hygroscopic than β-caryophyllene. It was suggested that the molecular weight of SOAs decreased with lower VOC molecular weight and may be more oxidized.[23] Additionally, fragmentation of aerosol particles into species such as low molecular weight carboxylic acids may further reduce the average molecular weight, increasing hygroscopicity.[23,24,28] The oxygenation level of SOAs varies with precursor concentration, OH sources, and exposure to light; however, under supersaturated conditions, apparent particle hygroscopicity was shown to be independent of O : C ratios, which is in clear contrast to subsaturated conditions where hygroscopicity has been reported to have a strong dependence on particle oxygenation.[29–33] Huff-Hartz *et al.* (2005) used a static diffusion cloud condensation nuclei counter (CCNC) to measure the activation diameter (dry particle size at which 50% of the particle population activate into droplets at a given supersaturation) of monoterpene and sesquiterpene SOAs and found that α-pinene SOA (VOC : ozone = 1 : 3) had an activation diameter that ranged between 120 nm and 140 nm at 0.3% supersaturation.[17]

In contrast, β-caryophyllene SOA (SOA : ozone = 1 : 2) had an activation diameter of 152 nm ± 26 nm at 1% supersaturation indicating that under these oxidation conditions, α-pinene SOA is significantly more hygroscopic than β-caryophyllene SOA.

Table 1 Summary of several previously reported values of κ_{CCNC} and κ_{HTDMA}

Reference	VOC	Chamber condition, oxidants, *etc.*	Seed	Technique	κ
Meyer *et al.* (2009)[16]	α-Pinene	NO_x, light	Ammonium sulfate	HTDMA	0.086
			—	HTDMA	0.026
Huff-Hartz *et al.* (2005)[17]	α-Pinene	O_3	—	CCNC	0.03–0.23
	β-Caryophyllene	O_3	—	CCNC	0.03–0.11
VanReken *et al.* (2005)[18]	α-Pinene	O_3	—	CCNC	0.014–0.091
Virkkula *et al.* (1999)[19]	α-Pinene	O_3	—	HTDMA	0.022
			Ammonium sulfate	HTDMA	0.04
Prenni *et al.* (2007)[20]	α-Pinene	O_3	—	HTDMA	0.022
			—	CCNC	0.1
Frosch *et al.* (2013)[15]	β-Caryophyllene	O_3	—	CCNC	0.026–0.048
Tang *et al.* (2012)[21]	β-Caryophyllene	O_3		CCNC	0.16–0.221
Asa-Awuku *et al.* (2009)[22]	β-Caryophyllene	O_3, 2-butanol	—	CCNC	0.017–0.040
Varutbangkul *et al.* (2006)[1]	α-Pinene	O_3, 50% RH	Ammonium sulfate	HTDMA	0.037
	β-Caryophyllene	O_3, 50% RH	—	HTDMA	0.009
Wang (2018)[23]	α-Pinene	O_3, UV, OH	Ammonium sulfate	CCNC	0.1
	β-Caryophyllene			CCNC	0.07
Engelhart (2008)[24]	α-Pinene	O_3	—	CCNC	0.14–0.16
Zhao (2016)	α-Pinene	O_3		HTDMA	0.03–0.06
				CCNC	0.1–0.15

However, Petters and Kreidenweis (2007) highlighted that κ_{CCNC} of α-pinene measured by Huff-Hartz *et al.* (2005) did not follow the lines of constant κ, which suggests that α-pinene SOA is only somewhat hygroscopic.[25] Work by Prenni *et al.*[20] (2007) also agrees with previous values, and reported κ_{CCNC} of α-pinene SOA to be 0.10 ± 0.04, and 0.02 under subsaturated conditions, which was in agreement with the work by Virkkula *et al.* (1999) which showed that the ozonolysis of α-pinene at 84% RH formed SOA with a growth factor (G_f) of 1.070, or $\kappa_{HTDMA} = 0.02$.[20,25,34]

To date, the literature has shown that the CCN activity of β-caryophyllene SOA can vary widely. For example, dark ozonolysis of β-caryophyllene SOA by Asa-Awuku *et al.* (2009) had a measured κ_{CCNC} between 0.02 and 0.04 in the presence of 2-butanol, which was within the range of κ-values reported by Huff-Hartz *et al.* (2005).[17,22] Tang *et al.* (2012) published κ_{CCNC} values for β-caryophyllene SOA to be between 0.25 and 0.27 in the absence of OH scavengers, and that light had negligible effects on β-caryophyllene SOA hygroscopicity.[21] Frosch *et al.* (2012) showed that β-caryophyllene SOA may increase hygroscopicity with oxidation, but this only marginally increased G_f. Under subsaturated conditions, HTDMA measurements of photochemically aged β-caryophyllene SOA at 90% RH (Frosch *et al.* (2012)) resulted in G_f between 1.00 and 1.09, and corresponds to κ_{HTDMA} of 0.00–0.03, which is close to κ_{CCNC} reported by Huff-Hartz *et al.* (2005).[15,17] Higher κ_{CCNC} measurements by Tang *et al.* (2012) could be primarily attributed to the low precursor concentrations of β-caryophyllene (5–20 ppb) and a larger reaction chamber which results in more hygroscopic and oxidized SOAs, whereas previous studies had between 25 and 100 ppb of the precursor and a smaller chamber.[21]

To further mimic the ambient atmosphere, the effect of inorganic seeds and humidity on α-pinene and β-caryophyllene SOAs has been the subject of several studies. Virkkula *et al.* (1999) used a Humidified Tandem Differential Mobility Analyzer (HTDMA) to measure the G_f of α-pinene SOA formed through dark ozonolysis at 84% RH, with and without the presence of ammonium sulfate seeds ($G_{f,ammonium\ sulfate} = 1.5$) and reported growth factors that corresponded to κHTDMA between 0.02 and 0.04, consistent with previous observations.[34,36–38] Two explanations were offered by Virkkula *et al.* (1999) on why SOAs from various precursors exhibit $G_f \sim 1.1$: the first is that the organic coating may be permeable and water molecules can access the inorganic core, or that the organic coating and inorganic core form a homogeneous mixture such that there is no clear distinction between the core and the organic coating.

Varutbangkul *et al.* (2006) explored the subsaturated water uptake at 85% RH of ammonium sulfate seeded α-pinene and unseeded β-caryophyllene SOAs formed through photooxidation in the presence of 50% RH in an SOA chamber.[1] α-pinene exhibited $\kappa_{HTDMA} = 0.037$ and β-caryophyllene was less hygroscopic with $\kappa_{HTDMA} = 0.009$. It was concluded that SOAs from both precursors are slightly hygroscopic, but less than inorganic salts such as ammonium sulfate, and show a continuous water uptake through a range of relative humidities with no deliquescence or efflorescence behavior. Furthermore, SOA hygroscopicity results from competing effects: further oxidation of organic products to more polar and hygroscopic species, or formation of larger and less hydrophilic oligomers. The CCN activity of seeded α-pinene and seeded β-caryophyllene SOAs has been shown to be close to κ_{HTDMA}.[39,40]

Previously mentioned studies mainly considered the water-uptake of SOAs formed under dry conditions (<10% RH), with the exception of Varutbangkul *et al.* (2006). It must be acknowledged that the presence of water vapor or high humidity during SOA formation may alter the yield, and physical and optical properties of aerosols. Recent studies indicated that SOAs formed at higher RH could have different physical and chemical properties, such as viscosity.[41] For example, Boyd *et al.* (2017) hypothesized that terpene SOA formed in the presence of 70% RH and nitrate radicals was viscous due to the low hygroscopicity of the SOA.[41] Additionally, Emanuelsson *et al.* (2013) showed that humidity during SOA formation increased aerosol volatility.[42] In addition, the work of Yuan *et al.* (2017) suggests that the formation of SOAs in the presence of water-vapor may form more stable Criegee-intermediates that could lead to the formation of more hygroscopic materials for monoterpene SOA systems.[43]

In this study, we focus our efforts towards understanding the differences in measured hygroscopicity that could result from modifying the initial water-vapor concentration in the reaction chamber. The difference in the extent to which SOA inorganic mixtures take up water formed under wet conditions is unknown. Furthermore, three hygroscopicity measurement platforms, previously shown to agree well for simple well-defined compositions,[6] are applied. Specifically, HTDMA and CNNC measurements have been aptly used to estimate particle water-uptake (Table 1). Fewer studies have used cavity ring-down spectroscopy (CRD) and similar methods to investigate SOAs. These studies have mainly focused on determining the refractive index (RI) of the systems of interest.[6,44–52] Denjean *et al.* (2015) used CRD to measure the hygroscopicity of α-pinene SOA and reported a growth factor between 1.020 and 1.070 ($\kappa = 0.003$–0.010), which agrees with other literature values.[20,44] In addition to refractive index measurements of SOAs, the generation of SOAs in the presence of NO_x has been studied frequently but only a few studies utilize CRD in their analysis.[53–56]

In summary, hygroscopicity of α-pinene and β-caryophyllene SOAs depends on SOA generation conditions (*i.e.*, concentration, oxidants, scavengers, humidity, *etc.*), and thus there is a need for continued research on the magnitude of these effects and their climatic implications.[1,16,21] This work highlights the focus on the potential differences observed with humidity during formation. In this research, *in situ* measurements of α-pinene and β-caryophyllene SOA hygroscopicities are performed under 4 SOA formation conditions: dry chamber (5% RH) unseeded, dry chamber with ammonium sulfate seeds, humid chamber (76% RH) unseeded, and humid chamber with ammonium sulfate seeds. Sub and supersaturated water uptake properties were measured using HTDMA, CRD, and CCNC, and compared using the single hygroscopicity parameter κ as introduced by Petters and Kreidenweis (2007).[25]

2 Materials and methods

2.1 SOA generation

Laboratory-generated SOA was produced with a 1 m^3 Tedlar chamber (Welch Fluorocarbon). Before each experiment, the chamber was cleaned with excess ozone (~100 ppm) and then purged with a continuous flow of purified air for 8 hours. Ozone was generated *via* a corona discharge tube ozone generator (Ozotech Inc. Poseidon 200). The chamber was first filled with purified air and ozone at the beginning of each experiment. The target ozone concentrations were between 200 ppb and 300 ppb and were sample-dependent (*vide infra*).

As previously mentioned, SOAs were generated under four chamber conditions: (1) dry unseeded SOA, (2) wet unseeded SOA, (3) dry SOA with ammonium sulfate seeds, and (4) wet SOA with ammonium sulfate seeds where dry conditions were defined as having an RH < 10% and wet conditions were defined as being between 75 and 80% RH. The humidification in the chamber was maintained at a level so as to prevent the deliquescence of ammonium sulfate particles in wet seeded experiments. It was assumed that RH in the chamber remained constant, and while changes in RH may modify the propensity of wall losses during SOA formation, we expect that effects on the intrinsic hygroscopicities are negligible. For humidification experiments, air was filtered downstream of a bubbler containing ultrapure water (Millipore™ water < 18 MΩ). For seeded experiments, ammonium sulfate was atomized into the reaction chamber until the particle counter read a total concentration of 25 000 ± 3000 particles per cm^3. Aerosol particles were created by atomizing a dilute solution of ammonium sulfate (100 mg L^{-1} ammonium sulfate, 98%, Fisher Chemical™) using a constant output atomizer (TSI 3076) with a 3.6 L min^{-1} carrier gas of purified air and dehydrating the polydisperse aerosol particles *via* a silica gel diffusion dryer (Fig. 1). Ammonium sulfate seed particles were added to the chamber under dry conditions.

Two volatile organic carbon precursors were then added to the well-mixed chamber system. Specifically, α-pinene (Aldrich™, 98%) and β-caryophyllene (Sigma™, >98.5%) were injected through the chamber's resealable entrance using a syringe onto a glass plate located at the base of the environmental chamber where VOCs rapidly volatilize to initiate nucleation and particle formation. α-Pinene SOA was generated using 200 ppb of ozone and 150 ppb of α-pinene and β-caryophyllene SOAs was formed in the presence of 400 ppb of ozone and 300 ppb of the β-caryophyllene precursor.

After VOC injection, SOA concentrations were monitored by using a Differential Mobility Analyzer (DMA, TSI 3081) and a condensation particle counter (CPC, TSI 3776). The DMA was set to mobility diameter scanning mode. Particles in the chamber were assumed to be well-mixed when the geometric mean of the distribution remained constant for over 30 minutes. Subsequently, SOA water uptake was measured by three separate hygroscopicity measurement techniques: cavity ring-down spectroscopy (CRD), humidified tandem differential mobility analysis (HTDMA), and cloud condensation nuclei counting (CCNC) that have been previously validated and detailed in Dawson *et al.* (2020), and will only be briefly described below.[6]

2.2 Cloud condensation nuclei droplet growth

The cloud condensation nuclei (CCN) activity was immediately measured after particle formation for each SOA experiment. The aerosol particles were dried upon exiting the chamber *via* a diffusion drier and subsequently sampled from the chamber for size distribution measurement by an electrostatic classifier in scanning mode. The aerosol sample was then split into two parallel streams. A condensation particle counter (CPC, TSI 3776) sampled at a flow rate of 0.3 L min^{-1} and measured the total particle concentration for a given size. Simultaneously, a continuous flow streamwise thermal gradient cloud condensation nuclei counter (CCNC; Droplet Measurement Technologies, DMT© CCN-100) sampled aerosol at 0.5 L min^{-1} and measured the CCN number concentration. The CCNC was calibrated with ammonium sulfate prior to experimental measurements. The aerosol size (from 8 to 352 nm) and CCN distribution was measured every 2 minutes and 15 seconds, and the CCN concentration was measured for a constant instrument supersaturation for ~10 minutes and supersaturation in the CCNC varied from 0.4% to 0.8% as the aerosol size distribution moved to larger sizes.

The critical activation diameter (D_d) is defined as the 50% efficiency of the ratio of CCN to total particle concentration. The scanning mobility CCN analysis (SMCA) method was used and has been previously used to measure α-pinene SOA and β-

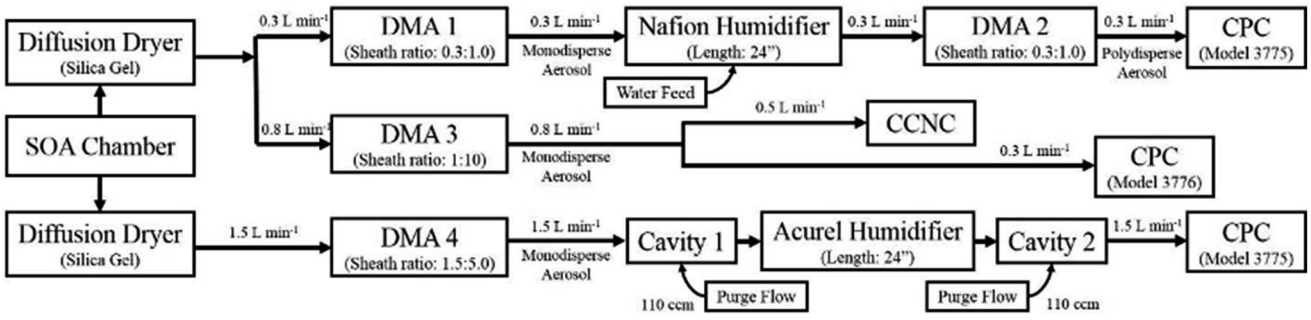

Fig. 1 Diagram of the experimental set-up consisting of three complementary methods: HTDMA, CCNC, and CRD.

caryophyllene SOA CCN activity.[21,24,28,57] Supersaturation and D_d data were used to calculate κ in the supersaturated RH regime based on κ-Köhler theory (Petters and Kreidenweis, 2007).[25]

2.3 Humidified tandem differential mobility droplet growth

Subsaturated geometric growth factors of the laboratory-generated SOA were measured with a HTDMA. The HTDMA is commonly used for aerosol hygroscopicity measurements and a detailed setup has been described in previous publications.[31,57–61] HTDMA sampling began approximately two hours after SOA particle formation, when sufficient aerosol had shifted to larger sizes (≥200 nm), as particle growth is more easily observed at these sizes.

As for CCN measurements, sampled dry aerosol particles are first separated by their electrical mobility diameter by using a differential mobility analyzer (DMA, TSI 3081). The sample to sheath flow was maintained at a ratio of 0.3 : 1.0 which allowed for the selection of dry particles (D_{dry}) of 200, 250, and 300 nm. The selected aerosols were then humidified by using a Nafion humidification line (PermaPure® MH series) to 95% RH. The humidified distribution was then measured with a scanning mobility particle sizer (SMPS, DMA TSI 3081/CPC TSI 3775). The geometric mean of the humidified distribution (D_{wet}) was then used to calculate the geometric growth factor as has been previously described using a simple geometric growth factor calculation.

$$G_f(\text{wet, dry}) = \frac{D_{wet}}{D_{dry}} \quad (1)$$

Similar HTDMA measurement techniques have measured α-pinene SOA and β-caryophyllene SOA.[1,16,20,31,35,39,44,62–65]

2.4 Cavity ring-down spectroscopy

The particles grew to sufficiently large sizes for CRD roughly three hours after SOA generation and one hour into HTDMA measurements. Again, the aerosol particles were dried upon exiting the chamber with a diffusion drier (Fig. 1). The sample was then size selected by using a differential mobility analyzer (DMA, TSI 3081) to obtain dry mobility diameters of 200 nm, 225 nm, 250 nm, 275 nm, 300 nm, 350 nm, and 400 nm. The aerosol to sheath flow ratio was set to 1.5 : 5.0 to maintain this range of particle mobility diameters without changing the sheath flow. The CRD setup in this research has previously been described in detail, and only a brief overview is presented here.[6,66] The CRD spectrometer measures extinction coefficients which are related to ring-down times according to

$$\alpha_{ext} = \frac{R_L}{c}\left(\frac{1}{\tau} - \frac{1}{\tau_0}\right) \quad (2)$$

where α_{ext} is the extinction efficiency, R_L is the length of the cavity, c is the speed of light, τ_0 is the ring-down time when no sample is in the cavity, and τ is the ring-down time when the sample is present. The refractive index of a sample can be determined by first calculating the experimental extinction cross-section (σ_{exp}) by dividing the average extinction coefficient ($\alpha_{exp,avg}$) by the average particle concentration (N_{avg})

$$\sigma_{exp} = \frac{\alpha_{exp,avg}}{N_{avg}} \quad (3)$$

The extinction cross section is related to the extinction efficiency (Q_{ext}) by

$$Q_{ext} = \frac{\sigma_{ext}}{\pi r^2} \quad (4)$$

where r is the particle radius. Using Mie theory, theoretical Q_{ext} was retrieved from a range of refractive indices and compared to the experimental value to determine the sample refractive index. The best-fit of the refractive index is one with the lowest reduced cumulative fractional difference (CFD_R)

$$CFD_R = \frac{1}{P}\sum_{\text{all sizes}} \frac{|\alpha_{ext,ave} - \alpha_{ext,Mie}|}{\alpha_{ext,ave}} \quad (5)$$

where $\alpha_{ext,Mie}$ is the theoretical extinction efficiency based on Mie theory and P is the number of selected sizes.

The CRD in this work consists of two cavities, a dry cavity and a humidified cavity. As size-selected aerosol particles are introduced into either cavity, the extinction of light by those particles is measured. The extinction of the humidified aerosol particles ($\sigma_{ext,a}$) was then divided by the extinction of the dry particles ($\sigma_{ext,b}$) to obtain an optical growth factor for each dry mobility size as shown by

$$f\text{RH}(a,b) = \frac{\sigma_{ext,a}}{\sigma_{ext,b}} \quad (6)$$

The optical growth factor (fRH) is then converted to the geometric growth factor using Mie scattering theory and the basis of eqn (1) where D_{dry} is the dry particle mobility diameter selected by the DMA, and D_{wet} is the diameter of the humidified particles derived from the humidified particle extinction coefficient and the refractive index of the particle. This method has been discussed before and is only briefly described here where extinction coefficients are calculated for the particle size every 0.1 nm above the original dry particle size until a calculated extinction coefficient is found that best matches the extinction coefficient of the humidified particle that was experimentally determined.[6,66] In the CRD chamber studies, the flow of the sample through the system is governed by the CPC (TSI 3775) which was operated at a 1.5 L min^{-1} flow rate. The actual flow from the chamber was slightly less than this value as each of the mirrors in the CRD had a purge flow of 40 cm^3 min^{-1} which was maintained across them throughout the experiment. Each measurement technique was calibrated with ammonium sulfate (Millipore™, 99%) aerosol particles which were generated using a constant output atomizer (TSI 3076).

2.5 Hygroscopicity analysis

The measured CCN activity, sub-saturated droplet growth, and optical growth can be converted to the hygroscopicity parameter, κ.[25] For each measurement method, κ retrieval has been

described in detail by Dawson *et al.* (2020) and only an overview will be provided here.[6]

κ-Values can be derived from G_f and RH measurements at relative humidities (>80%), where the vapor pressure of water approaches that of a flat surface and droplet water activity can be approximated with RH. At RH > 80%, G_f can be simplified to ref. 67

$$G_f^3 = 1 + \kappa \frac{\mathrm{RH}/100}{1 - \mathrm{RH}/100} \quad (7)$$

and for supersaturated CCN measurement, κ is calculated *via*[25]

$$\kappa = \frac{4\left(\frac{4\sigma_{s/a} M_w}{RT\rho_w}\right)^3}{27 D_d^3 \ln^2 s} \quad (8)$$

where $\sigma_{s/a}$ is the surface tension of the droplet at the air droplet interface and is assumed to be that of pure water, D_d is the critical activation particle diameter, s is the instrument supersaturation, R is the universal gas constant, T is the temperature of the droplet, and M_w and ρ_w are the molecular weight and density of water, respectively.[25,67] Henceforth, we refer to κ-values derived from eqn (7) and (8) as κ_{HTDMA} and κ_{CCNC}, respectively.

The equations for single hygroscopicity optical growth measurements have not been explicitly derived. Previous studies have proposed two and three empirical parameter relationships between *f*RH and RH.[67–69] In this research, two techniques were employed to obtain κ-values from *f*RH data. The first method converts the optical growth factor to the geometric growth factor (G_f) using Mie theory and the experimentally derived refractive indices. The conversion to κ can thus use eqn (7).[69] The second *f*RH method applies an empirical relationship to solve for G_f, and is shown in eqn (9).[67]

$$\kappa_{CRD,emp} = \left(f\mathrm{RH}(80\%\ \mathrm{RH}, \mathrm{dry})^{3\times 0.28/0.86} - 1\right)\left(\frac{1 - \mathrm{RH}/100}{\mathrm{RH}/100}\right) \quad (9)$$

where $\kappa_{CRD,emp}$ is the empirically derived κ-value.[67] Here the distinction is made between κ-factors determined by Mie theory and that determined semi-empirically as $\kappa_{CRD,Mie}$ and $\kappa_{CRD,emp}$, respectively. $\kappa_{CRD,Mie}$ has been shown to be particle size-independent, and $\kappa_{CRD,emp}$ exhibits a similar size dependence to *f*RH data.[6] $\kappa_{CRD,emp}$ approaches κ-values of known aerosol compounds at larger particle sizes and both values have been shown to estimate slightly higher values than κ_{CCNC} and κ_{HTDMA} for water-soluble organic sugars.[6]

2.6 Estimation by the ZSR model and droplet growth predictions

The Zdanovskii–Stokes–Robinson (ZSR) model has been used to estimate the κ-value of aerosol mixtures based on the volume fraction (ε_i) and κ-value of each component (eqn (10)).[16,70–72]

$$\kappa = \sum_i \varepsilon_i \kappa_i \quad (10)$$

In this research, information on the volume fraction of the inorganic seeds (ammonium sulfate) and the SOA was directly obtained from the chamber. For each precursor, two ZSR estimations were done, one under supersaturated conditions, and one under subsaturated conditions, as κ-values are known to vary across the two saturation regimes.[25,27,62] κ_{CCNC} values of dry and wet unseeded α-pinene and β-caryophyllene SOAs (measured in this study) were used for supersaturated ZSR calculations. The subsaturated κ-values (κ_{HTDMA}, $\kappa_{CRD,Mie}$ and $\kappa_{CRD,emp}$) derived in this study were averaged for the subsaturated ZSR calculations. Particle growth was predicted based on the κ-Köhler theory with limited solubility considerations described in Petters and Kreidenweis (2008) and shown in eqn (11) where $H(x_i)$ is the dissolved volume fraction.[73]

$$\kappa = \sum \varepsilon_i \kappa_i H(x_i) \quad (11)$$

The solubility of monoterpene and sesquiterpene SOAs was assumed to be 0.1 g g^{-1} H_2O as reported by Huff-Hartz *et al.* (2005), and density of the SOAs was assumed to be 1.5 g cm^{-3}.[17,24]

3 Results and discussion

The presence of water vapor at subsaturated relative humidity may alter the formation and composition of α-pinene and β-caryophyllene SOAs, and may subsequently alter the SOA's water uptake properties. In this study, the effect of humidity on α-pinene and β-caryophyllene SOA water uptake is measured under sub- and supersaturated conditions and is presented in Fig. 2. Error bars represent the standard deviation of κ over three trials of each experiment.

A summary of measured κ-values is presented in Table S1.† The presence of water vapor during the formation of the α-pinene SOA did not appear to have a significant effect on the geometric growth factor derived κ_{HTDMA} values which were measured to be 0.059 and 0.042 without and with the presence of water vapor in the chamber, respectively. We discuss our measurements in the context of previous studies that have explored similar systems. Furthermore, we note and acknowledge the limits of the comparison with previous studies that have sometimes used different initial conditions in their studies. Varutbangkul *et al.* (2006) reported κ_{HTDMA} values of 0.055 and 0.021 for α-pinene and β-caryophyllene SOAs formed *via* ozonolysis in the presence of 50% RH, respectively. Juranyi *et al.* (2009) published a concentration-dependent κ_{HTDMA} of 0.07–0.13 for α-pinene SOA formed *via* photooxidation in the presence of NO_x and 50–60% RH. Two κ values were retrieved from CRD experiments, one based on the calculations by Kreidenweis and Asa-Awuku (2014) ($\kappa_{CRD,emp}$) and one from the methods described in previous literature ($\kappa_{CRD,Mie}$).[66,67] For $\kappa_{CRD,Mie}$ and $\kappa_{CRD,emp}$ reported in this study, the presence of water vapor enhanced measured κ values by 0.040, however, this difference is within the experimental error.

In contrast, humid conditions in the SOA chamber led to a notable difference in α-pinene SOA supersaturated water

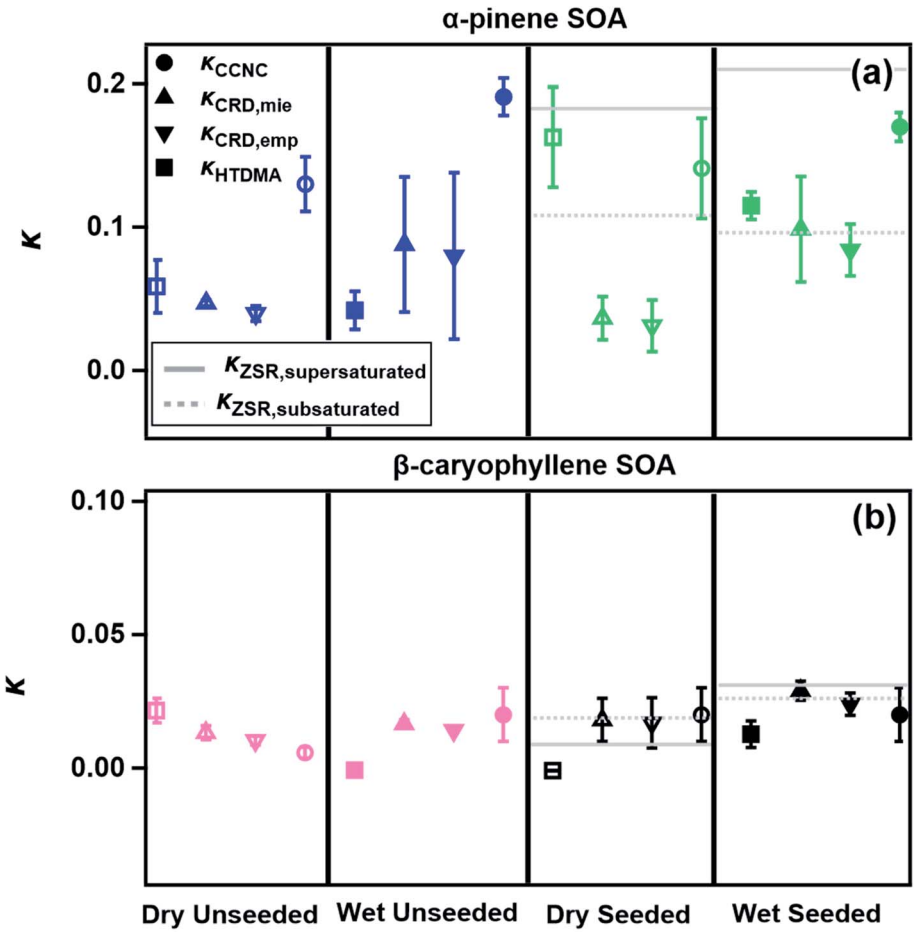

Fig. 2 κ_{HTDMA} (square), $\kappa_{CRD,Mie}$ (triangle), $\kappa_{CRD,emp}$ (inverted triangle), and κ_{CCNC} (circle) of (a) unseeded (blue) and ammonium sulfate seeded (green) α-pinene SOA and (b) unseeded (red) and ammonium sulfate seeded (black) β-caryophyllene SOA under dry (open symbols) and wet (filled symbols) SOA chamber conditions. Grey lines represent the predicted κ based on the ZSR model for supersaturated conditions (solid), and subsaturated conditions (dashed) for the seeded systems. Error bars signify one standard deviation. Note the change in y-axes from α-pinene to β-caryophyllene SOA.

uptake. Fig. 2a shows that the dry unseeded α-pinene SOA κ_{CCNC} value is 0.130 ± 0.019 as measured over the course of the experiment. κ_{CCNC} is notably higher compared to subsaturated κ, and increases from 0.130 to 0.191 under dry and wet chamber conditions (Fig. 2a). Measured water uptake and resulting κ-values of dry and wet unseeded α-pinene SOA under supersaturated and subsaturated conditions were consistent with previously reported values of α-pinene SOA.[17,24,28,29,39,62,63]

Fig. 2b shows that β-caryophyllene SOA is between non-hygroscopic to very slightly hygroscopic, as the measured κ values were nominally small (less than 0.1). It was also observed that the presence of ~70% RH during SOA formation did not significantly affect the measured κ. The two methods of κ retrievals from CRD resulted in invariable $\kappa_{CRD,Mie}$ and $\kappa_{CRD,emp}$. κ_{HTDMA} of dry and wet unseeded β-caryophyllene SOA exhibited a noticeable difference, although values were nominally small (Fig. 2b). Additionally, κ_{HTDMA} of wet unseeded β-caryophyllene SOA indicated that the SOA was non-hygroscopic.[74] Under supersaturated conditions, β-caryophyllene SOA was slightly hygroscopic ($\kappa_{CCNC,dry\text{-}unseeded} = 0.006$ and $\kappa_{CCNC\ wet\text{-}unseeded} = 0.020$), and the presence of water vapor during SOA formation increased κ_{CCNC} over threefold. Overall, however, β-caryophyllene SOA was effectively non-hygroscopic under experimental conditions. Additionally, measured β-caryophyllene κ_{CCNC} values were comparable to the reported values by Huff-Hartz *et al.* (2005) and Frosch *et al.* (2013), but were significantly less than the values reported by Tang *et al.* (2012) which may be due to differences in SOA formation experimental chamber conditions (Tang *et al.* (2012) used a low concentration of the precursor and a larger chamber).[15,17,21]

Four κ-values were calculated from the data collected in the experiments above and from the known solute parameters. It was assumed that the composition of aerosol particles remains constant and uniform throughout the measured size distribution. However, it is noted that the acquisition of these results occurs over the course of ~2 hours during which time the aerosol particles continuously interact with one another and grow.

κ-Values of aerosol mixtures retrieved from CRD measurements were in good agreement with each other, and the optical

growth factors are listed in Table S2.† This agreement suggests that the $\kappa_{CRD,emp}$ method is viable and can be applied to inorganics, organics, and mixed inorganic and organic fractions. In general, the κ-values derived from the CRD were lower than those from other methods (Fig. 2). This result is likely due to the lower RH within the system (85% RH). κ_{HTDMA} values were often in agreement with the other technique that operated in the subsaturated regime, CRD. It should be noted that in the case of the dry seeded α-pinene SOA, the κ_{HTDMA} value was closer to the value of κ_{CCNC} (Fig. 2). We propose that it is likely that seeded α-pinene SOA was fully deliquesced at RH_{HTDMA}, as shown by the κ_{HTDMA} value that was better predicted by the supersaturated ZSR model, whereas full deliquescence was not reached at RH_{CRD}, and particle growth was similar to that of dry, unseeded α-pinene SOA (Fig. 2).

κ_{CCNC} values were often higher than either the CRD or HTDMA-derived κ-values which is likely a result of the supersaturated conditions of the experiment, and is a trend that has occurred in previous studies.[6,25] This result is not surprising since the core principle of the droplet formation is the

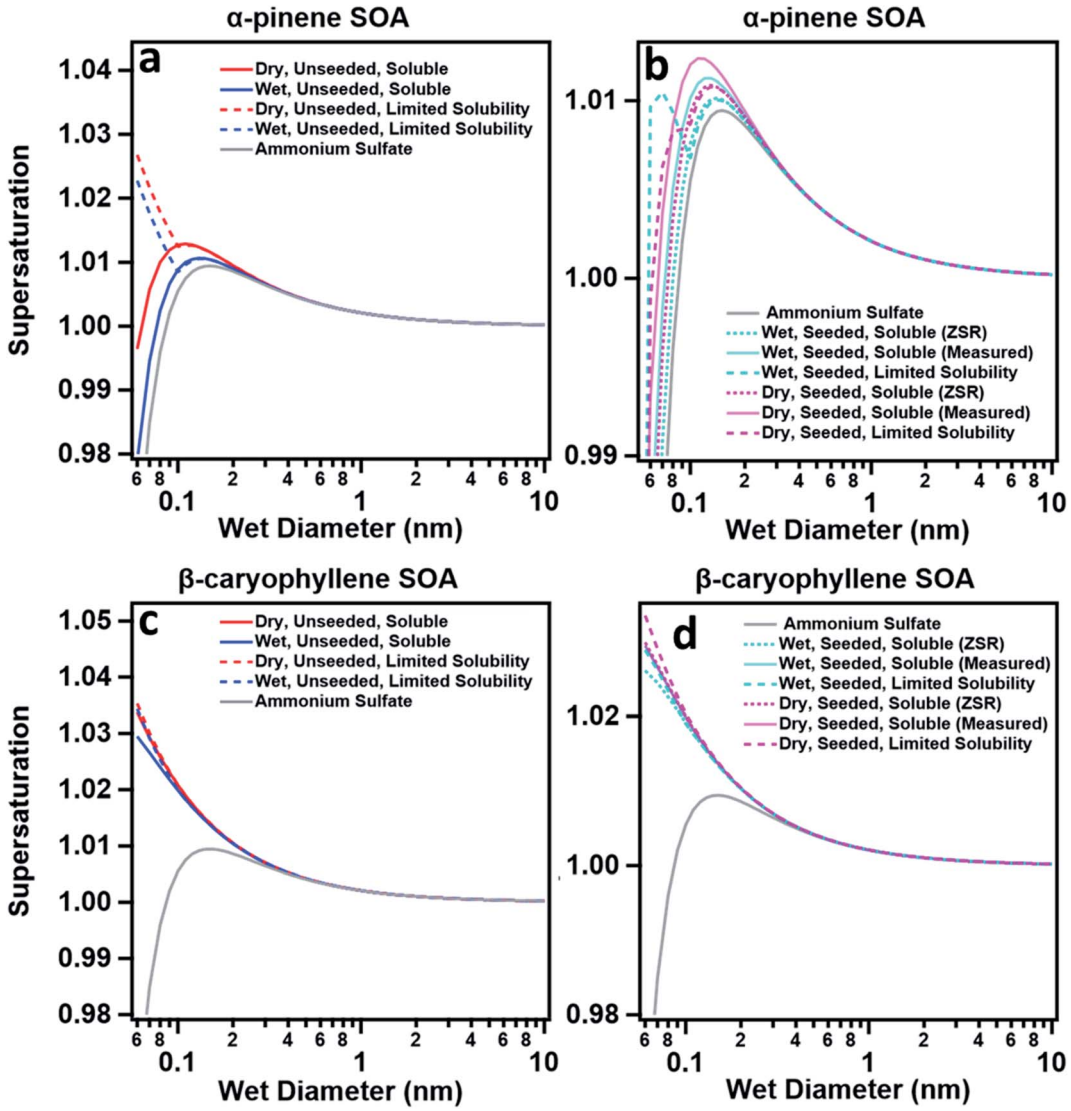

Fig. 3 Droplet growth predictions for α-pinene (a and b) and β-caryophyllene (c and d) under dry unseeded (red), wet unseeded (blue), dry seeded (magenta), and wet seeded (cyan) conditions. Particle growth was predicted under the assumption of infinite solubility (solid line), and limited solubility (dashed line). For seeded experiments, κ_{ZSR} was also used to model particle water uptake (dotted line). The solid grey line depicts the Kohler curve for ammonium sulfate. α-Pinene SOA water uptake is predicted to be affected by the organic solubility in water, which explains the difference between measured subsaturated and supersaturated κ-values. In the dry and wet seeded cases, ZSR slightly overestimates the water uptake and particle growth of α-pinene SOA. Accounting for limited solubility, dry seeded α-pinene SOA behaves like fully deliquesced aerosols whereas the growth of wet seeded α-pinene SOA is shown to be governed by the water uptake of the SOA in the model. It is noteworthy that the two critical supersaturation in the limited solubility wet seeded α-pinene SOA model are close in value, and may experimentally behave like soluble aerosols. As both wet and dry seeded α-pinene SOAs behave like fully deliquesced particles, the difference in inorganic volume fractions does not significantly affect particle growth.

generation of water vapor in a state far from equilibrium: the supersaturated water vapor will condense onto particles, where it can be more readily absorbed.

In general, the β-caryophyllene SOA exhibited little to no hygroscopic growth regardless of the experiment type and despite the presence of very hygroscopic ammonium sulfate in some of the experiments (Fig. 2b). It is likely that the β-caryophyllene SOA (in dry and wet experiments) coated the ammonium sulfate seeds, and completely inhibited water uptake by the core.

The α-pinene SOA exhibited a change in hygroscopicity when generated under humid conditions. Seeding the SOA with ammonium sulfate resulted in a key observation: at lower RH (<90%) the addition of ammonium sulfate seeds did not increase the hygroscopicity (Fig. 2a). As for the β-caryophyllene SOA, this is likely due to the SOA thoroughly coating the seed and inhibiting water uptake. However, with the techniques that operated at higher RH (>95% RH, *e.g.*, HTDMA, CCNC), the α-pinene SOA did exhibit an increase in hygroscopicity with the addition of ammonium sulfate seeds. In contrast, the β-caryophyllene with ammonium sulfate seeds did not. It has been shown that α-pinene SOA deliquesces around 90–95% RH and therefore when humidified past this point, the water would have access to the core, resulting in increased hygroscopic growth. κ-Kohler theory was used to predict the droplet growth of α-pinene and β-caryophyllene SOAs (Fig. 3).

For β-caryophyllene SOA, the models show that aerosol particles are nonhygroscopic – consistent with the experimental findings in Fig. 2. The ZSR model captured the measured κ of the non-hygroscopic β-caryophyllene but overestimated the supersaturated and subsaturated κ of seeded α-pinene SOA (Fig. 2). κ_{CCNC} values of dry seeded and unseeded α-pinene SOAs were invariant. When κ_{CCNC} of dry unseeded α-pinene SOA was used to calculate the seeded ZSR hygroscopicity, the ZSR model agreed with the measured κ_{CCNC} which supports the conclusion that the core and shell independently took up water. Therefore, hygroscopicity can be well predicted based on the volume fraction of the SOA and the ammonium sulfate core.

In summary, κ-values of α-pinene SOA are comparable and within the range of previously published literature values (despite the variation in the setup and initial conditions).[16,19,20,39] Presence of water vapor during α-pinene SOA formation did not significantly change its water uptake under subsaturated and supersaturated conditions. However, α-pinene SOA water uptake under subsaturated and supersaturated conditions is significantly different, and this difference may be associated with the solubility of the organic particles in water (Fig. 3). Lastly, supersaturated particle growth of seeded and unseeded α-pinene SOAs is invariant and is consistent with the values reported by Wang *et al.* (2018), Engelhart *et al.* (2008), and Zhao *et al.* (2016).[23,24,27] This agreement further suggests that α-pinene SOA behaves like fully deliquesced aerosols and that the presence of inorganic seed in the concentrations used does not greatly affect supersaturated particle growth. β-Caryophyllene SOA across all experiments was effectively non-hygroscopic and did not readily take up water. The agreement of α-pinene SOA systems with ZSR suggests that the slightly soluble and moderately hygroscopic α-pinene SOA aerosol deliquesces in droplet solution. Particles containing organic fractions that readily deliquesce have better agreement with ZSR. In other words, slightly soluble SOAs formed in the presence of water vapor facilitates droplet growth. Additionally, for slightly soluble, seeded particles instruments are sensitive to RH and presence of highly hygroscopic species. This is in contrast with the work of Dawson *et al.* (2020) where κ_{HTDMA}, κ_{CRD}, and κ_{CCNC} were in agreement when used to measure the water uptake of water soluble organic compounds.[6] Lastly, it must be acknowledged that there may be a temporal dependence of κ as measurements were conducted asynchronously; however, measured κ-values in the scope of this research was consistent with the literature values that have evaluated κ at various timeframes, and were not the source of variation in this research.[16,75]

4 Summary and implications

SOAs can take up water, changing both their direct and indirect optical properties. Using three complementary techniques we determined the κ-values for laboratory-generated SOAs. Here, the differences between measured κ-values for the α-pinene and β-caryophyllene SOAs are measured on three separate aerosol hygroscopicity platforms. The results also emphasize the importance of composition on hygroscopicity and the differences that may result with varying water-vapor initial conditions. When water-vapor is the only gas-phase initial concentration varied, the relative importance for subsequent aerosol hygroscopicity is highlighted. This research adds to the growing body of work that advocates for the use of two or more hygroscopicity measurement methods for mixed aerosols. Seeded particles did not grow in the HTDMA, CRD, and CCNC when the organic coating did not likely deliquesce. Recent work suggests that inhibition of water uptake of SOAs is likely due to limited solubility and viscosity of SOAs.[76–83] β-Caryophyllene SOA formed under either dry or humid conditions is less soluble and more hydrophobic and more viscous than α-pinene SOA.[76] Therefore, in all experiments β-caryophyllene SOA did not show changes in hygroscopicity. α-Pinene SOA physical properties are dependent on relative humidity; for seeded α-pinene SOA, once the deliquescence point of the SOA has been reached, the ammonium sulfate core is free to take up water. This suggests that the type of mixed organic–inorganic aerosols that occur in tropical regions and sub-tropical summer times (high RH) may have different water-uptake properties than mixed aerosols in arid (low RH) regions or dry winters, particularly with aerosol compositions of majority monoterpene rather than sesquiterpene SOA. Hygroscopicity of aerosol particles plays an important role in the determination of their optical properties and the formation of clouds and haze. The results reported in this work may be able to reduce the errors in water-uptake and climate models.

Author contributions

AAA, TMR, DDD, MAF, KAM, PNR, and JND designed and performed the HTDMA experiments. JND, KD and MAF designed and performed the CRD experiments. AAA, TMR, DDD, KAM

and PNR designed and performed the CCN experiments. PNR did the calculations using the H-TDMA and CCN data. JND, KD, and MAF performed the calculations using the CRD data. PNR prepared the manuscript with input from all the co-authors.

Conflicts of interest

The authors declare that they have no conflict of interest.

Acknowledgements

MAF and JND acknowledge support from the NSF: AGS-1723290. JND acknowledges funding from the NSF GRFP (NSF 1255832). AAA and PNR acknowledge support from the NSF: AGS-1723920. DDD, TMR, and KAM acknowledge support from the NSF: 1723874.

References

1 V. Varutbangkul, F. J. Brechtel, R. Bahreini, N. L. Ng, M. D. Keywood, J. H. Kroll, R. C. Flagan, J. H. Seinfeld, A. Lee and A. H. Goldstein, Hygroscopicity of secondary organic aerosols formed by oxidation of cycloalkenes, monoterpenes, sesquiterpenes, and related compounds, *Atmos. Chem. Phys.*, 2006, **6**, 2367–2388.

2 T. F. Stocker, D. Qin, G.-K. Plattner, L. V. Alexander, S. K. Allen, N. L. Bindoff, F.-M. Bréon, J. A. Church, U. Cubasch, S. Emori, P. Forster, P. Friedlingstein, N. Gillett, J. M. Gregory, D. L. Hartmann, E. Jansen, B. Kirtman, R. Knutti, K. Krishna Kumar, P. Lemke, J. Marotzke, V. Masson-Delmotte, G. A. Meehl, I. I. Mokhov, S. Piao, V. Ramaswamy, D. Randall, M. Rhein, M. Rojas, C. Sabine, D. Shindell, L. D. Talley, D. G. Vaughan and S.-P. Xie, Technical Summary, in *Climate Change 2013: The Physical Science Basis. Contribution of Working Group I to the Fifth Assessment Report of the Intergovernmental Panel on Climate Change*, ed. T. F.Stocker, D. Qin, G.-K. Plattner, M. Tignor, S. K. Allen, J. Boschung, A. Nauels, Y. Xia, V. Bex and P. M. Midgley, Cambridge University Press, Cambridge, United Kingdom and New York, NY, USA, 2013.

3 IPCC, Summary for Policymakers, in *Climate Change 2013: The Physical Science Basis. Contribution of Working Group I to the Fifth Assessment Report of the Intergovernmental Panel on Climate Change*, ed. T. F. Stocker, D. Qin, G.-K. Plattner, M. Tignor, S. K. Allen, J. Boschung, A. Nauels, Y. Xia, V. Bex and P. M. Midgley, Cambridge University Press, Cambridge, United Kingdom and New York, NY, USA, 2013.

4 NARSTO, *Particulate Matter Science for Policy Makers: A NARSTO Assessment*, ed. P. McMurry, M. Shepherd, and J. Vickery, Cambridge University Press, Cambridge, England, 2004, ISBN 0 52 184287 5.

5 D. Rose, S. S. Gunthe, E. Mikhailov, G. P. Frank, U. Dusek, M. O. Andreae and U. Pöschl, Calibration and measurement uncertainties of a continuous-flow cloud condensation nuclei counter (DMT-CCNC): CCN activation of ammonium sulfate and sodium chloride aerosol particles in theory and experiment, *Atmos. Chem. Phys.*, 2008, **8**, 1153–1179.

6 J. N. Dawson, K. A. Malek, P. N. Razafindrambinina, T. M. Raymond, D. D. Dutcher, A. A. Asa-Awuku and M. A. Freedman, Direct Comparison of the Submicron Aerosol Hygroscopicity of Water-Soluble Sugars, *ACS Earth Space Chem.*, 2020, **4**(12), 2215–2226.

7 Q. Zhang, J. L. Jimenez, M. R. Canagaratna, J. D. Allan, H. Coe, I. Ulbrich, M. R. Alfarra, A. Takami, A. M. Middlebrook, Y. L. Sun, K. Dzepina, E. Dunlea, K. Docherty, P. F. Decarlo, D. Salcedo, T. Onasch, J. T. Jayne, T. Miyoshi, A. Shimono, S. Hatakeyama, N. Takegawa, Y. Kondo, J. Schneider, F. Drewnick, L. Cottrell, R. J. Griffin, J. Rautiainen, J. Y. Sun and Y. M. Zhang, Ubiquity and dominance of oxygenated species in organic aerosols in anthropogenically-influenced Northern Hemisphere midlatitudes, *Geophys. Res. Lett.*, 2007, **34**, L13801.

8 G. T. Wolff, M. S. Ruthkosky, D. P. Stroup and P. E. Korsog, A characterization of the principal PM-10 species in Claremont (summer) and Long Beach (fall) during SCAQS, *Atmos. Environ., Part A*, 1991, **25**, 2173–2186.

9 C. S. Sloane, J. Watson, J. Chow, L. Pritchett and L. Willard Richards, Size-segregated fine particle measurements by chemical species and their impact on visibility impairment in Denver, *Atmos. Environ., Part A*, 1991, **25**, 1013–1024.

10 J. C. Chow, J. G. Watson, E. M. Fujita, Z. Lu, D. R. Lawson and L. L. Ashbaugh, Temporal and spatial variations of PM2.5 and PM10 aerosol in the Southern California air quality study, *Atmos. Environ.*, 1994, **28**, 2061–2080.

11 B. J. Turpin, J. J. Huntzicker, S. M. Larson and G. R. Cass, Los Angeles Summer Midday Particulate Carbon: Primary and Secondary Aerosol, *Environ. Sci. Technol.*, 1991, **25**, 1788–1793.

12 H. Zhang, L. D. Yee, B. H. Lee, M. P. Curtis, D. R. Worton, G. Isaacman-VanWertz, J. H. Offenberg, M. Lewandowski, T. E. Kleindienst, M. R. Beaver, A. L. Holder, W. A. Lonneman, K. S. Docherty, M. Jaoui, H. O. T. Pye, W. Hu, D. A. Day, P. Campuzano-Jost, J. L. Jimenez, H. Guo, R. J. Weber, J. De Gouw, A. R. Koss, E. S. Edgerton, W. Brune, C. Mohr, F. D. Lopez-Hilfiker, A. Lutz, N. M. Kreisberg, S. R. Spielman, S. V. Hering, K. R. Wilson, J. A. Thornton and A. H. Goldstein, Monoterpenes are the largest source of summertime organic aerosol in the southeastern United States, *Proc. Natl. Acad. Sci. U. S. A.*, 2018, **115**, 2038–2043.

13 R. J. Griffin, D. R. Cocker III, J. H. Seinfeld and D. Dabdub, Estimate of global atmospheric organic aerosol from oxidation of biogenic hydrocarbons, *Geophys. Res. Lett.*, 1999, **26**, 2721–2724.

14 M. Kanakidou, J. H. Seinfeld, S. N. Pandis, I. Barnes, F. J. Dentener, M. C. Facchini, R. Van Dingenen, B. Ervens, A. Nenes, C. J. Nielsen, E. Swietlicki, J. P. Putaud, Y. Balkanski, S. Fuzzi, J. Horth, G. K. Moortgat, R. Winterhalter, C. E. L. Myhre, K. Tsigaridis, E. Vignati, E. G. Stephanou and J. Wilson, Organic aerosol and global

climate modelling: A review, *Atmos. Chem. Phys.*, 2005, **5**, 1053–1123.

15 M. Frosch, M. Bilde, A. Nenes, A. P. Praplan, Z. Jurányi, J. Dommen, M. Gysel, E. Weingartner and U. Baltensperger, *Atmos. Chem. Phys.*, 2013, **13**, 2283–2297.

16 N. K. Meyer, J. Duplissy, M. Gysel, A. Metzger, J. Dommen, E. Weingartner, M. R. Alfarra, A. S. H. Prevot, C. Fletcher, N. Good, G. McFiggans, A. M. Jonsson, M. Hallquist, U. Baltensperger and Z. D. Ristovski, Analysis of the hygroscopic and volatile properties of ammonium sulphate seeded and unseeded SOA particles, *Atmos. Chem. Phys.*, 2009, **9**, 721–732.

17 K. E. Huff Hartz, T. Rosenørn, S. R. Ferchak, T. M. Raymond, M. Bilde, N. M. Donahue and S. N. Pandis, Cloud condensation nuclei activation of monoterpene and sesquiterpene secondary organic aerosol, *J. Geophys. Res., D: Atmos.*, 2005, **110**, 1–8.

18 T. M. VanReken, N. L. Ng, R. C. Flagan and J. H. Seinfeld, Cloud condensation nucleus activation properties of biogenic secondary organic aerosol, *J. Geophys. Res.: Atmos.*, 2005, **110**, 1–9.

19 A. Virkkula, R. Van Dingenen, F. Raes and J. Hjorth, Hygroscopic properties of aerosol formed by oxidation of limonene, α-pinene, and β-pinene, *J. Geophys. Res.: Atmos.*, 1999, **104**, 3569–3579.

20 A. J. Prenni, M. D. Petters, S. M. Kreidenweis, P. J. DeMott and P. J. Ziemann, Cloud droplet activation of secondary organic aerosol, *J. Geophys. Res.: Atmos.*, 2007, DOI: 10.1029/2006JD007963.

21 X. Tang, D. R. Cocker and A. Asa-Awuku, Are sesquiterpenes a good source of secondary organic cloud condensation nuclei (CCN)? Revisiting β-caryophyllene CCN, *Atmos. Chem. Phys.*, 2012, **12**, 8377–8388.

22 A. Asa-Awuku, G. J. Engelhart, B. H. Lee, S. N. Pandis and A. Nenes, Relating CCN activity, volatility, and droplet growth kinetics of β-caryophyllene secondary organic aerosol, *Atmos. Chem. Phys.*, 2009, **9**, 795–812.

23 J. Wang, J. Shilling, J. Liu, A. Zelenyuk, D. Bell, M. Petters, R. Thalman, F. Mei, R. Zaveri and G. Zheng, Cloud droplet activation of secondary organic aerosol is mainly controlled by molecular weight, not water solubility, *Atmos. Chem. Phys. Discuss.*, 2018, **19**, 1–34.

24 G. J. Engelhart, A. Asa-Awuku, A. Nenes and S. N. Pandis, CCN activity and droplet growth kinetics of fresh and aged monoterpene secondary organic aerosol, *Atmos. Chem. Phys.*, 2008, **8**, 3937–3949.

25 M. D. Petters and S. M. Kreidenweis, A single parameter representation of hygroscopic growth and cloud condensation nucleus activity, *Atmos. Chem. Phys.*, 2007, **7**, 1961–1971.

26 H. Köhler, The nucleus in and the growth of hygroscopic droplets, *Trans. Faraday Soc.*, 1936, **32**, 1152–1161.

27 D. F. Zhao, A. Buchholz, B. Kortner, P. Schlag, F. Rubach, H. Fuchs, A. Kiendler-Scharr, R. Tillmann, A. Wahner, K. Watne, M. Hallquist, J. M. Flores, Y. Rudich, K. Kristensen, A. M. K. Hansen, M. Glasius, I. Kourtchev, M. Kalberer and T. F. Mentel, Cloud condensation nuclei activity, droplet growth kinetics, and hygroscopicity of biogenic and anthropogenic secondary organic aerosol (SOA), *Atmos. Chem. Phys.*, 2016, **16**, 1105–1121.

28 A. T. Lambe, T. B. Onasch, P. Massoli, D. R. Croasdale, J. P. Wright, A. T. Ahern, L. R. Williams, D. R. Worsnop, W. H. Brune and P. Davidovits, Laboratory studies of the chemical composition and cloud condensation nuclei (CCN) activity of secondary organic aerosol (SOA) and oxidized primary organic aerosol (OPOA), *Atmos. Chem. Phys.*, 2011, **11**, 8913–8928.

29 M. Frosch, M. Bilde, P. F. DeCarlo, Z. Jurányi, T. Tritscher, J. Dommen, N. M. Donahue, M. Gysel, E. Weingartner and U. Baltensperger, Relating cloud condensation nuclei activity and oxidation level of α-pinene secondary organic aerosols, *J. Geophys. Res.: Atmos.*, 2011, **116**, 1–9.

30 L. Poulain, Z. Wu, M. D. Petters, H. Wex, E. Hallbauer, B. Wehner, A. Massling, S. M. Kreidenweis and F. Stratmann, Towards closing the gap between hygroscopic growth and CCN activation for secondary organic aerosols-Part 3: Influence of the chemical composition on the hygroscopic properties and volatile fractions of aerosols, *Atmos. Chem. Phys.*, 2010, **10**, 3775–3785.

31 J. Duplissy, P. F. De Carlo, J. Dommen, M. R. Alfarra, A. Metzger, I. Barmpadimos, A. S. H. Prevot, E. Weingartner, T. Tritscher, M. Gysel, A. C. Aiken, J. L. Jimenez, M. R. Canagaratna, D. R. Worsnop, D. R. Collins, J. Tomlinson and U. Baltensperger, Relating hygroscopicity and composition of organic aerosol particulate matter, *Atmos. Chem. Phys.*, 2011, **11**, 1155–1165.

32 T. Tritscher, J. Dommen, P. F. Decarlo, M. Gysel, P. B. Barmet, A. P. Praplan and E. Weingartner, Physics Volatility and Hygroscopicity of Aging Secondary Organic Aerosol in a Smog Chamber, *Atmos. Chem. Phys.*, 2011, 11477–11496.

33 J. L. Jimenez, M. R. Canagaratna, N. M. Donahue, A. S. H. Prevot, Q. Zhang, J. H. Kroll, P. F. DeCarlo, J. D. Allan, H. Coe, N. L. Ng, A. C. Aiken, K. S. Docherty, I. M. Ulbrich, A. P. Grieshop, A. L. Robinson, J. Duplissy, J. D. Smith, K. R. Wilson, V. A. Lanz, C. Hueglin, Y. L. Sun, J. Tian, A. Laaksonen, T. Raatikainen, J. Rautiainen, P. Vaattovaara, M. Ehn, M. Kulmala, J. M. Tomlinson, D. R. Collins, M. J. Cubison, J. Dunlea, J. A. Huffman, T. B. Onasch, M. R. Alfarra, P. I. Williams, K. Bower, Y. Kondo, J. Schneider, F. Drewnick, S. Borrmann, S. Weimer, K. Demerjian, D. Salcedo, L. Cottrell, R. Griffin, A. Takami, T. Miyoshi, S. Hatakeyama, A. Shimono, J. Y. Sun, Y. M. Zhang, K. Dzepina, J. R. Kimmel, D. Sueper, J. T. Jayne, S. C. Herndon, A. M. Trimborn, L. R. Williams, E. C. Wood, A. M. Middlebrook, C. E. Kolb, U. Baltensperger and D. R. Worsnop, Evolution of Organic Aerosols in the Atmosphere, *Science*, 2009, **326**, 1525–1529.

34 A. Virkkula, R. Van Dingenen, F. Raes and J. Hjorth, *J. Geophys. Res.: Atmos.*, 1999, **104**, 3569–3579.

35 M. R. Alfarra, J. F. Hamilton, K. P. Wyche, N. Good, M. W. Ward, T. Carr, M. H. Barley, P. S. Monks,

M. E. Jenkin, A. C. Lewis and G. B. McFiggans, *Atmos. Chem. Phys.*, 2012, **12**, 6417–6436.

36 K. Hämeri, M. Rood and H. C. Hansson, Hygroscopic properties of a NaCl aerosol coated with organic compounds, *J. Aerosol Sci.*, 1992, **23**, 437–440.

37 H. C. Hansson, A. Wiedensohler, M. J. Rood and D. S. Covert, Experimental determination of the hygroscopic properties of organically coated aerosol particles, *J. Aerosol Sci.*, 1990, **21**, 241–244.

38 C. N. Cruz and S. N. Pandis, The effect of organic coatings on the cloud condensation nuclei activation of inorganic atmospheric aerosol, *J. Geophys. Res.: Atmos.*, 1998, **103**, 13111–13123.

39 Z. Jurányi, M. Gysel, J. Duplissy, E. Weingartner, T. Tritscher, J. Dommen, S. Henning, M. Ziese, A. Kiselev, F. Stratmann, I. George and U. Baltensperger, Influence of gas-to-particle partitioning on the hygroscopic and droplet activation behaviour of α-pinene secondary organic aerosol, *Phys. Chem. Chem. Phys.*, 2009, **11**, 8091–8097.

40 S. M. King, T. Rosenoern, J. E. Shilling, Q. Chen and S. T. Martin, Cloud condensation nucleus activity of secondary organic aerosol particles mixed with sulfate, *Geophys. Res. Lett.*, 2007, **34**, 1–5.

41 C. M. Boyd, T. Nah, L. Xu, T. Berkemeier and N. L. Ng, Secondary Organic Aerosol (SOA) from Nitrate Radical Oxidation of Monoterpenes: Effects of Temperature, Dilution, and Humidity on Aerosol Formation, Mixing, and Evaporation, *Environ. Sci. Technol.*, 2017, **51**, 7831–7841.

42 E. U. Emanuelsson, Å. K. Watne, A. Lutz, E. Ljungström and M. Hallquist, Influence of humidity, temperature, and radicals on the formation and thermal properties of secondary organic aerosol (SOA) from ozonolysis of β-Pinene, *J. Phys. Chem. A*, 2013, **117**, 10346–10358.

43 C. Yuan, Y. Ma, Y. Diao, L. Yao, Y. Zhou, X. Wang and J. Zheng, *J. Geophys. Res.*, 2017, **122**, 4654–4669.

44 C. Denjean, P. Formenti, B. Picquet-Varrault, E. Pangui, P. Zapf, Y. Katrib, C. Giorio, A. Tapparo, A. Monod, B. Temime-Roussel, P. Decorse, C. Mangeney and J. F. Doussin, *Atmos. Chem. Phys.*, 2015, **15**, 3339–3358.

45 M. S. Ugelow, K. J. Zarzana, D. A. Day, J. L. Jimenez and M. A. Tolbert, The optical and chemical properties of discharge generated organic haze using in situ real-time techniques, *Icarus*, 2017, **294**, 1–13.

46 C. A. Hasenkopf, M. R. Beaver, M. G. Trainer, H. Langley Dewitt, M. A. Freedman, O. B. Toon, C. P. McKay and M. A. Tolbert, Optical properties of Titan and early Earth haze laboratory analogs in the mid-visible, *Icarus*, 2010, **207**, 903–913.

47 N. Bluvshtein, P. Lin, J. Michel Flores, L. Segev, Y. Mazar, E. Tas, G. Snider, C. Weagle, S. S. Brown, A. Laskin and Y. Rudich, Broadband optical properties of biomass-burning aerosol and identification of brown carbon chromophores, *J. Geophys. Res.*, 2017, **122**, 5441–5456.

48 D. Kwon, V. W. Or, M. J. Sovers, M. Tang, P. D. Kleiber, V. H. Grassian and M. A. Young, Optical Property Measurements and Single Particle Analysis of Secondary Organic Aerosol Produced from the Aqueous-Phase Reaction of Ammonium Sulfate with Methylglyoxal, *ACS Earth Space Chem.*, 2018, **2**, 356–365.

49 T. Nakayama, K. Sato, Y. Matsumi, T. Imamura, A. Yamazaki and A. Uchiyama, Wavelength dependence of refractive index of secondary organic aerosols generated during the ozonolysis and photooxidation of α-pinene, *Sci. Online Lett. Atmosphere*, 2012, **8**, 119–123.

50 Q. He, N. Bluvshtein, L. Segev, D. Meidan, J. M. Flores, S. S. Brown, W. Brune and Y. Rudich, Evolution of the Complex Refractive Index of Secondary Organic Aerosols during Atmospheric Aging, *Environ. Sci. Technol.*, 2018, **52**, 3456–3465.

51 J. M. Flores, D. F. Zhao, L. Segev, P. Schlag, A. Kiendler-Scharr, H. Fuchs, A. K. Watne, N. Bluvshtein, T. F. Mentel, M. Hallquist and Y. Rudich, Evolution of the complex refractive index in the UV spectral region in ageing secondary organic aerosol, *Atmos. Chem. Phys.*, 2014, **14**, 5793–5806.

52 K. J. Zarzana, D. O. De Haan, M. A. Freedman, C. A. Hasenkopf and M. A. Tolbert, Optical properties of the products of α-dicarbonyl and amine reactions in simulated cloud droplets, *Environ. Sci. Technol.*, 2012, **46**, 4845–4851.

53 T. Nakayama, K. Sato, Y. Matsumi, T. Imamura, A. Yamazaki and A. Uchiyama, Wavelength and NO_x dependent complex refractive index of SOAs generated from the photooxidation of toluene, *Atmos. Chem. Phys.*, 2013, **13**, 531–545.

54 T. Nakayama, K. Sato, M. Tsuge, T. Imamura and Y. Matsumi, Complex refractive index of secondary organic aerosol generated from isoprene/NO_x photooxidation in the presence and absence of SO_2, *J. Geophys. Res.*, 2015, **120**, 7777–7787.

55 R. M. Varma, S. M. Ball, T. Brauers, H. P. Dorn, U. Heitmann, R. L. Jones, U. Platt, D. Pöhler, A. A. Ruth, A. J. L. Shillings, J. Thieser, A. Wahner and D. S. Venables, Light extinction by secondary organic aerosol: an intercomparison of three broadband cavity spectrometers, *Atmos. Meas. Tech.*, 2013, **6**, 3115–3130.

56 X. Qi, S. Zhu, C. Zhu, J. Hu, S. Lou, L. Xu, J. Dong and P. Cheng, Smog chamber study of the effects of NO_x and NH_3 on the formation of secondary organic aerosols and optical properties from photo-oxidation of toluene, *Sci. Total Environ.*, 2020, **727**, 138632.

57 R. H. Moore and A. Nenes, Scanning flow CCN analysis a method for fast measurements of CCN spectra, *Aerosol Sci. Technol.*, 2009, **43**, 1192–1207.

58 C. N. Cruz and S. N. Pandis, Deliquescence and hygroscopic growth of mixed inorganic – Organic atmospheric aerosol, *Environ. Sci. Technol.*, 2000, **34**, 4313–4319.

59 D. J. Rader and P. H. McMurry, Application of the tandem differential mobility analyzer to studies of droplet growth or evaporation, *J. Aerosol Sci.*, 1986, **17**, 771–787.

60 E. Swietlicki, H. C. Hansson, K. Hämeri, B. Svenningsson, A. Massling, G. Mcfiggans, P. H. Mcmurry, T. Petäjä, P. Tunved, M. Gysel, D. Topping, E. Weingartner, U. Baltensperger, J. Rissler, A. Wiedensohler and

M. Kulmala, Hygroscopic properties of submicrometer atmospheric aerosol particles measured with H-TDMA instruments in various environments – A review, *Tellus, Ser. B: Chem. Phys. Meteorol.*, 2008, **60**, 432–469.

61 N. F. Taylor, D. R. Collins, C. W. Spencer, D. H. Lowenthal, B. Zielinska, V. Samburova and N. Kumar, Measurement of ambient aerosol hydration state at Great Smoky Mountains National Park in the southeastern United States, *Atmos. Chem. Phys.*, 2011, **11**, 12085–12107.

62 H. Wex, M. D. Petters, C. M. Carrico, E. Hallbauer, A. Massling, G. R. McMeeking, L. Poulain, Z. Wu, S. M. Kreidenweis and F. Stratmann, Towards closing the gap between hygroscopic growth and activation for secondary organic aerosol: Part 1-Evidence from measurements, *Atmos. Chem. Phys.*, 2009, **9**, 3987–3997.

63 P. Massoli, A. T. Lambe, A. T. Ahern, L. R. Williams, M. Ehn, J. Mikkilä, M. R. Canagaratna, W. H. Brune, T. B. Onasch, J. T. Jayne, T. Petäjä, M. Kulmala, A. Laaksonen, C. E. Kolb, P. Davidovits and D. R. Worsnop, Relationship between aerosol oxidation level and hygroscopic properties of laboratory generated secondary organic aerosol (SOA) particles, *Geophys. Res. Lett.*, 2010, **37**, 1–5.

64 J. F. Hamilton, M. R. Alfarra, K. P. Wyche, M. W. Ward, A. C. Lewis, G. B. McFiggans, N. Good, P. S. Monks, T. Carr, I. R. White and R. M. Purvis, Investigating the use of secondary organic aerosol as seed particles in simulation chamber experiments, *Atmos. Chem. Phys.*, 2011, **11**, 5917–5929.

65 J. Duplissy, M. Gysel, S. Sjogren, N. Meyer, N. Good and L. Kammermann, Intercomparison study of six HTDMAs: results and general recommendations for HTDMA operation, *Atmos. Meas. Tech. Discuss.*, 2008, **1**, 127–168.

66 D. P. Veghte, M. B. Altaf, J. D. Haines and M. A. Freedman, Optical properties of non-absorbing mineral dust components and mixtures, *Aerosol Sci. Technol.*, 2016, **50**, 1239–1252.

67 S. M. Kreidenweis and A. Asa-Awuku, *Aerosol Hygroscopicity: Particle Water Content and its Role in Atmospheric Processes*, 2014.

68 C. D. Cappa, D. L. Che, S. H. Kessler, J. H. Kroll and K. R. Wilson, Variations in organic aerosol optical and hygroscopic properties upon heterogeneous OH oxidation, *J. Geophys. Res.: Atmos.*, 2011, **116**, 1–12.

69 R. M. Garland, A. R. Ravishankara, E. R. Lovejoy, M. A. Tolbert and T. Baynard, Parameterization for the relative humidity dependence of light extinction: Organic-ammonium sulfate aerosol, *J. Geophys. Res.: Atmos.*, 2007, **112**, 1–11.

70 W. Xu, K. N. Fossum, J. Ovadnevaite, C. Lin, R. Huang, C. O. Dowd and D. Ceburnis, The impact of aerosol size-dependent hygroscopicity and mixing state on the cloud condensation nuclei potential over the Northeast Atlantic, *Atmos. Chem. Phys. Discuss.*, 2021, 1–31.

71 B. Jing, S. Tong, Q. Liu, K. Li, W. Wang, Y. Zhang and M. Ge, Hygroscopic behavior of multicomponent organic aerosols and their internal mixtures with ammonium sulfate, *Atmos. Chem. Phys.*, 2016, **16**, 4101–4118.

72 B. Svenningsson, J. Rissler, E. Swietlicki, M. Mircea, M. Bilde, M. C. Facchini, S. Decesari, S. Fuzzi, J. Zhou, J. Mønster and T. Rosenørn, Hygroscopic growth and critical supersaturations for mixed aerosol particles of inorganic and organic compounds of atmospheric relevance, *Atmos. Chem. Phys.*, 2006, **6**, 1937–1952.

73 M. D. Petters and S. M. Kreidenweis, A single parameter representation of hygroscopic growth and cloud condensation nucleus activity – Part 2: including solubility, *Atmos. Chem. Phys.*, 2008, **8**, 6273–6279.

74 T. Lei, A. Zuend, W. G. Wang, Y. H. Zhang and M. F. Ge, Hygroscopicity of organic compounds from biomass burning and their influence on the water uptake of mixed organic ammonium sulfate aerosols, *Atmos. Chem. Phys.*, 2014, **14**, 11165–11183.

75 A. E. Vizenor and A. A. Asa-Awuku, Gas-phase kinetics modifies the CCN activity of a biogenic SOA, *Phys. Chem. Chem. Phys.*, 2018, **20**, 6591–6597.

76 A. M. Maclean, N. R. Smith, Y. Li, Y. Huang, A. P. S. Hettiyadura, G. V. Crescenzo, M. Shiraiwa, A. Laskin, S. A. Nizkorodov and A. K. Bertram, Humidity-Dependent Viscosity of Secondary Organic Aerosol from Ozonolysis of β-Caryophyllene: Measurements, Predictions, and Implications, *ACS Earth Space Chem.*, 2021, **5**, 305–318.

77 A. Tandon, N. El Rothfuss and M. Petters, The effect of hydrophobic glassy organic material on the cloud condensation nuclei activity of internally mixed particles with different particle morphologies, *Atmos. Chem. Phys. Discuss.*, 2018, 1–24.

78 E. J. E. Ott, E. C. Tackman and M. A. Freedman, Effects of Sucrose on Phase Transitions of Organic/Inorganic Aerosols, *ACS Earth Space Chem.*, 2020, **4**, 591–601.

79 T. Koop, J. Bookhold, M. Shiraiwa and U. Pöschl, Glass transition and phase state of organic compounds: dependency on molecular properties and implications for secondary organic aerosols in the atmosphere, *Phys. Chem. Chem. Phys.*, 2011, **13**, 19238–19255.

80 B. Zobrist, V. Soonsin, B. P. Luo, U. K. Krieger, C. Marcolli, T. Peter and T. Koop, Ultra-slow water diffusion in aqueous sucrose glasses, *Phys. Chem. Chem. Phys.*, 2011, **13**, 3514–3526.

81 E. Mikhailov, S. Vlasenko, S. T. Martin, T. Koop and U. Pöschl, Amorphous and crystalline aerosol particles interacting with water vapor: conceptual framework and experimental evidence for restructuring, phase transitions and kinetic limitations, *Atmos. Chem. Phys.*, 2009, **9**, 9491–9522.

82 M. Shiraiwa, L. D. Yee, K. A. Schilling, C. L. Loza, J. S. Craven, A. Zuend, P. J. Ziemann and J. H. Seinfeld, Size distribution dynamics reveal particle-phase chemistry in organic aerosol formation, *Proc. Natl. Acad. Sci. U. S. A.*, 2013, **110**, 11746–11750.

83 B. J. Murray, Inhibition of ice crystallisation in highly viscous aqueous organic acid droplets, *Atmos. Chem. Phys.*, 2008, **8**, 5423–5433.